

Multi-scale Protocol for Mechanistic Reaction Studies Using Semi-local Fitted Potential Energy Surfaces

Tomislav Piskor,^{*,†,‡} Peter Pinski,[†] Thilo Mast,[†] and Vladimir V. Rybkin[†]

[†]*HQS Quantum Simulations GmbH, Rintheimer Strasse 23, 76131 Karlsruhe, Germany*

[‡]*Theoretical Physics, Saarland University, 66123 Saarbrücken, Germany*

E-mail: tomislav.piskor@quantumsimulations.de

Abstract

In this work, we propose a multi-scale protocol for routine theoretical studies of chemical reaction mechanisms. The initial reaction paths of our investigated systems are sampled using the Nudged-Elastic Band (NEB) method driven by a cheap electronic structure method. Forces recalculated at the more accurate electronic structure theory for a set of points on the path are fitted with a machine-learning technique (in our case symmetric gradient domain machine learning or sGDML) to produce a semi-local reactive Potential Energy Surface (PES), embracing reactants, products and transition state (TS) regions. This approach has been successfully applied to a unimolecular (Bergman cyclization of enediyne) and a bimolecular (S_N2 substitution) reaction. In particular, we demonstrate that with only 50 to 150 energy-force evaluations with the accurate reference methods (here CASSCF and CCSD) it is possible to construct a semi-local PES giving qualitative agreement for stationary-point geometries, intrinsic reaction-coordinates and barriers. Furthermore, we find a qualitative agreement in vibrational frequencies and reaction rate coefficients. The key aspect of the method's

performance is its multi-scale nature, which not only saves computational effort but also allows extracting meaningful information along the reaction path, characterized by zero gradients in all but one direction. Agnostic to the nature of the TS and computationally economic, the protocol can be readily automated and routinely used for mechanistic reaction studies.

1 Introduction

Mechanistic studies of chemical reactions are one of the most important and wide-spread applications of computational quantum chemistry.¹ A minimal meaningful workflow consists of locating reactants, products and a corresponding transition state (TS). This allows one to assess the thermodynamics and kinetics of reactions *without* thermal contributions and thereby reveal reaction mechanisms. It is highly desirable to perform vibrational analysis for stationary points of a Potential Energy Surface (PES) to elucidate whether the structures correspond to minima or saddle points. This also allows to compute reaction rate coefficients via canonical Transition-State Theory (TST) taking vibrational degrees of freedom into account.² To be more rigorous, one should also compute reaction paths connecting the stationary points, one option being following the Intrinsic Reaction Coordinate (IRC) starting from the TS.³

These objectives are routinely reached by direct dynamics approaches,⁴ *i.e.* methods evaluating energy and its derivatives on-the-fly. The number of *ab initio* quantum chemistry calls typically reaches hundreds and more. One should not ignore unsuccessful attempts to locate TS and find IRC, which are not uncommon for mechanistic reaction studies. Qualitatively accurate descriptions of reactions involving the breaking or forming of chemical bonds can only be achieved with correlated electronic structure methods. Often but not always those include static correlation, *i.e.* multi-reference and multi-configurational approaches.⁵ Such methods are, however, computationally demanding even for moderate-size systems. Therefore, researchers often apply computationally cheaper methods for mechanistic reac-

tion studies, applying more accurate electronic structure theories only to stationary points (for example see the study of the reaction between ferrocenium and trimethylphosphine⁶). This creates inconsistencies and is a source of errors. Thus, it is desirable to recycle the results of expensive calculations by fitting the PES in relevant parts of the configuration space. Once a fitted PES is available, one can complete many tasks “free” of charge, including reactive molecular dynamics simulations, canonical and variational TST calculations,² etc.

A fitted PES can be efficiently generated using one of the rapidly evolving Machine-Learning (ML) approaches (for the general method overviews see review⁷ and perspective⁸). These typically require little if any feature design taking structures-energy (energy gradient) pairs as input. They demonstrate remarkable flexibility, successfully describing even non-adiabatic processes^{9,10} and systems without a classical atomistic structural formula.¹¹ The main type of application for such ML-PES is extensive Molecular Dynamics (MD) sampling (see exemplary applications to organic crystals¹² and liquid water¹³). The resulting PES is often called “global” as it embraces vast regions of the configuration space, although the reactive regions of it are typically not covered. There are only a handful of applications of ML-PES fitting to reactive systems: second-order nucleophilic substitution (S_N2),¹⁴ pericyclic,¹⁵ decomposition,¹⁶ dissociation,¹⁷ Diels-Alder¹⁸ and proton-transfer reactions.¹⁹ In addition, ML-PES have been successfully used for automatic mechanism discovery.²⁰ All these applications, however, aimed at “global” PES fitting required abundant data: typical sets include at least thousands of data points. Most of them, therefore, used Density Functional Theory (DFT) methods or cheaper many-body correlated wave functions as underlying electronic structure theory.

To facilitate routine mechanistic reaction studies one should be able to construct semi-local reactive PES with only a few hundreds of data points using high-level *ab initio* methods. Such work has been performed by Young *et al.*²¹ for several model processes, although the authors restricted themselves to DFT methods, which are typically insufficient to describe

chemical reactions due to their single-reference character.

In this work we propose a multi-scale protocol for generating semi-local reactive PES for routine mechanistic reaction studies based on ML methods with small data sets and a combination of electronic structure theories. Computationally cheaper DFT is used to generate relevant structures, whereas high-level *ab initio* methods are applied to refine the energetics. The multi-level nature of the protocol makes it suitable for incorporating evolving quantum computing methods which promise quantum advantage for correlated electronic-structure problems,²² while remaining non-routine. The feasibility of the approach is demonstrated with two organic reactions: monomolecular Bergman cyclization of enediyne to para-benzyne²³ and a bimolecular S_N2 reaction of chloromethane with a bromide ion.²⁴ The former is a textbook example of a chemical reaction involving multi-reference character²⁵ and is treated with a complete-active-space self-consistent-field method, whereas the latter can be described with a single-reference correlated method²⁶ and is treated with a coupled-cluster approach.

This paper is organized as follows. In section 2, we introduce the simulation protocol. In particular, we focus on obtaining relevant geometries for the investigated reactions, as well as reference methods and the machine learning technique of choice. Next, we present the results: PES sections, energy and force-prediction errors, and performance of the ML-PES for geometry optimization, vibrations and reaction rates. We conclude and give an outlook for this work in section 5 and refer to the supporting information, which gives details about the used parameters.

2 Methodology

2.1 Simulation protocol

We applied the general protocol for fitting a semi-local reactive PES, which includes the following steps:

1. Optimize reactants and products with a cheaper electronic structure method;
2. Find an approximate reaction path using the Nudged Elastic Band (NEB) method²⁷ with a cheaper electronic structure method;
3. Select points along the reaction path to form the data set;
4. Calculate energies and forces with a reference correlated method;
5. Split this data set into training, validation and test subsets;
6. Fit the ML-PES, validate and test using the corresponding subsets.

After being generated, the fitted PES was employed to compute the properties: stationary points, harmonic vibrations and intrinsic reaction coordinates in both directions from the TS. In addition, we calculated rate coefficients using transition state theory (TST). To evaluate the quality of the fitted semi-local PES the properties were compared with those obtained directly by the reference electronic structure method with energies and forces calculated on-the-fly.

The details of each step are described below.

2.2 Electronic structure calculations

We used DFT with the PBE exchange-correlation functional²⁸ in combination with the double-zeta split-valence def2-SVP basis set²⁹ as a cheaper electronic structure method for both reactions. These calculations have been performed with NWChem.³⁰

For the Bergman cyclization the complete active space self-consistent field (CASSCF)³¹ method with the double-zeta split-valence def2-SVP basis set²⁹ was used as the reference. For the initial configuration, we used MP2 natural orbitals to select the active space guess, which consisted of 12 electrons in 12 orbitals (12, 12) made of all carbon p-orbitals. The CASSCF wave function for atomic configurations in the data set was calculated with the

previous guess for the molecular orbitals, so that no discontinuities occurred in the potential energy surface. CASSCF calculations were performed using PySCF.^{32,33}

The reference correlated method for the S_N2 reaction was coupled-cluster singles and doubles (CCSD)³⁴ based on the Hartree-Fock reference within the spin-restricted formalism. As in the previous example, CCSD calculations have been performed with PySCF.³³ The basis set of choice has been the double-zeta correlation-consistent basis set cc-PVDZ.³⁵⁻³⁷

2.3 Data set generation

NWChem³⁰ has been used to generate the data sets by performing NEB²⁷ calculations. For both reactions, DFT (the cheaper method) energies and forces were used, with reactants as start points and products as end points. We used 100 beads for the S_N2 reaction and 200 for the Bergman cyclization. The geometries were randomly selected from the optimized elastic band. Thus, they lie on the approximate transition path of the PES obtained from the cheaper method, rather than on the path of the reference method.

2.4 Machine learning fit of the semi-local reactive PES

We opted for the symmetric gradient domain machine learning (sGDML) method³⁸⁻⁴⁰ to fit the PES as it efficiently employs the forces and does not require feature design: sGDML uses inverse atomic distances as features and the interatomic forces as the output. Importantly, sGDML has been shown to faithfully reproduce PES from a limited number of structures. Moreover, it has been successfully applied to small molecules using coupled-cluster reference data.⁴¹

To perform one sGDML fit, a certain number of points from the data set is taken to define the training, validation and test set. These numbers are detailed in section 3. The first step within one sGDML run is to generate a first model by constructing the kernel matrix out of the training points and setting values for the hyper-parameters σ and λ . The regularization parameter is hereby fixed to a certain value and the length scale σ is varied during the

learning process. After the training step, the model is validated against the validation set, where the energy and gradient errors are determined. This procedure is continued until the best σ is found. As a last step the optimized model is validated against the test set, which has no data from neither the training nor validation set and the errors in energy and gradients are compared.

2.5 Property calculation

We optimized the stationary points of the PES using DFT-optimized structures as initial guess and followed the IRC from the TS in both directions with `pysisyphus`.⁴² Both, the fitted PES and the reference electronic structure method in `PySCF`³³ were employed as energy functions. Gradients for both PES types were calculated analytically.

We calculated harmonic vibrations for all stationary points on the PES and computed the reaction rate coefficients using conventional TST with a harmonic oscillator-rigid rotor approximation for the partition functions. The working equations and the corresponding rates are given in the Supporting Information (Section 1).

3 Results

In this section, we present the results for our investigated examples. At first, the PES scans for the reference method and sGDML, as well as the energy differences between both methods will be shown. The next analysis will provide information about the mean absolute errors of the geometries between the reference and machine learning method for the reactant and TS. To perform geometry optimizations for both structures, we used the open-source package `pysisyphus`. In addition, we computed and compared harmonic vibrations for the optimized structures. Besides the intrinsic reaction coordinate we finally compared the reaction rate coefficients for all methods and reactions. The intrinsic reaction coordinate has been determined with `pysisyphus` as well, where the Euler-Predictor-Corrector integrator

was used.

3.1 Bergman cyclization of enediyne

The reaction is shown in Fig. 1, including the optimized reactant and product.

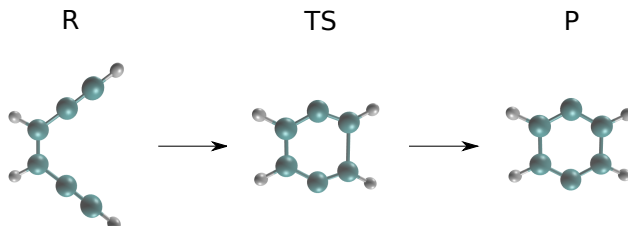


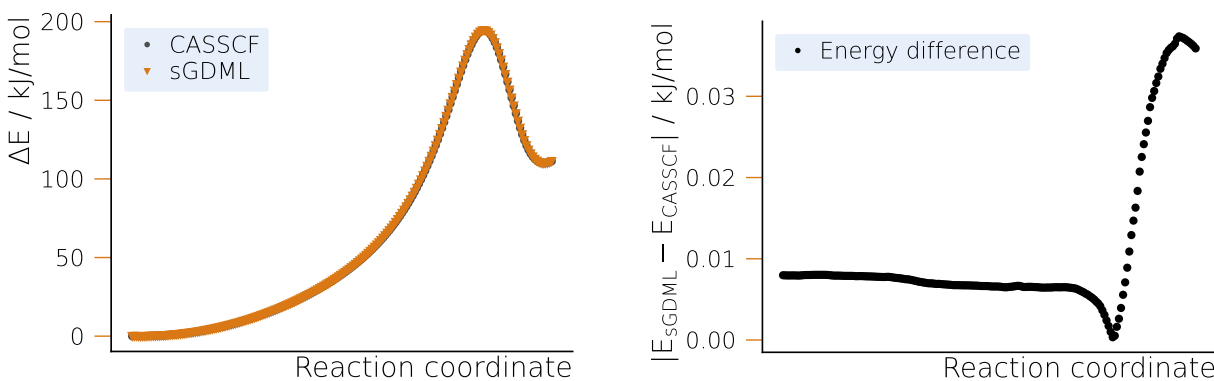
Figure 1: Bergman cyclization of enediyne. The reactant, transition state and product are labeled with R, TS, and P, respectively. Elements are colored as follows: carbon (cyan), hydrogen (white).

3.1.1 Model training

We created an sGDML model for the data set consisting of 200 data points: we used 150 training, 30 validation and 20 test points. The regularization parameter was set to $\lambda = 10^{-15}$ and the best length scale was found to be $\sigma = 6$. With these parameters, we obtained a model with a Mean Absolute Error (MAE) of 0.0067 kJ/mol and a Root Mean Square Error (RMSE) of 0.0071 kJ/mol for the energy, whereas the MAE and RMSE for the forces was 0.0033 kJ/Å · mol and 0.0075 kJ/Å · mol, respectively.

3.1.2 Potential energy surface scan

The PES profiles corresponding to the DFT optimized NEB path computed with CASSCF and sGDML are shown in Fig. 2a. As expected from the small values of MAE and RMSE, the two surfaces agree within chemical accuracy (see Fig. 2b). Starting from the reactant state and moving towards the TS the energy error is small and practically constant. The smallest error can be found in the vicinity of the TS, increasing significantly towards the product state, although still being two orders of magnitude within chemical accuracy.



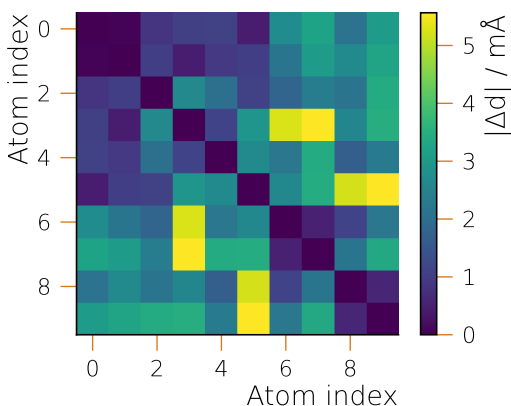
(a) Potential energy surface for CASSCF and sGDML.

(b) Energy differences between the learned and CASSCF potential energy surface.

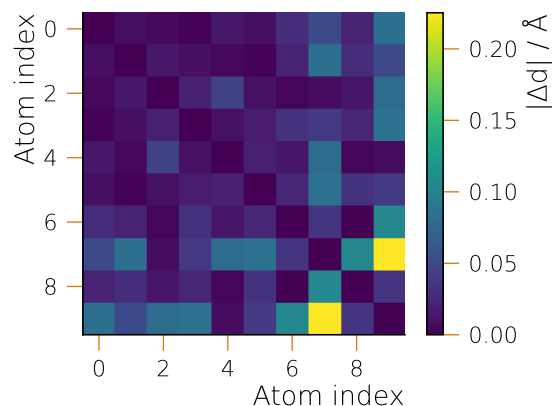
Figure 2: Potential energy profile for the Bergman cyclization of enediyne along the optimized NEB path.

3.1.3 Geometry optimization

In Fig. 3a we compare the geometric structures of the reactant and TS as obtained by sGDML and the reference method, CASSCF. Directly comparing the optimized geometries from both methods, we find that the MAE for all inter-atomic distances never reaches the value of 0.01 Å for the reactant state. However, for the TS, the error is considerably larger reaching a deviation of 0.22 Å in the worst case. Although it is a significant value, the corresponding distance is between two non-bonded hydrogen atoms separated by more than 5 Å. For other distances, the error does not exceed 0.1 Å.



(a) Geometry differences (MAE) for sGDML and CASSCF after performing geometry optimizations for the reactant state.



(b) Geometry differences (MAE) for sGDML and CASSCF after performing geometry optimizations for the transition state.

Figure 3: Accuracy of geometric structures from the semi-local fitted PES for the Bergman cyclization of enediyne.

3.1.4 Vibrations, intrinsic reaction coordinates and reaction rate coefficients

After obtaining the optimized TS, we analyze the connection between it and the basins of reactants and products by integrating the IRC as shown in Fig. 4. On the fitted semi-local PES, the TS does connect the reactants and products by a minimum energy path, which is in qualitative agreement with the reference CASSCF calculation along the entire curve as indicated by the maximum and RMS errors in the gradients.

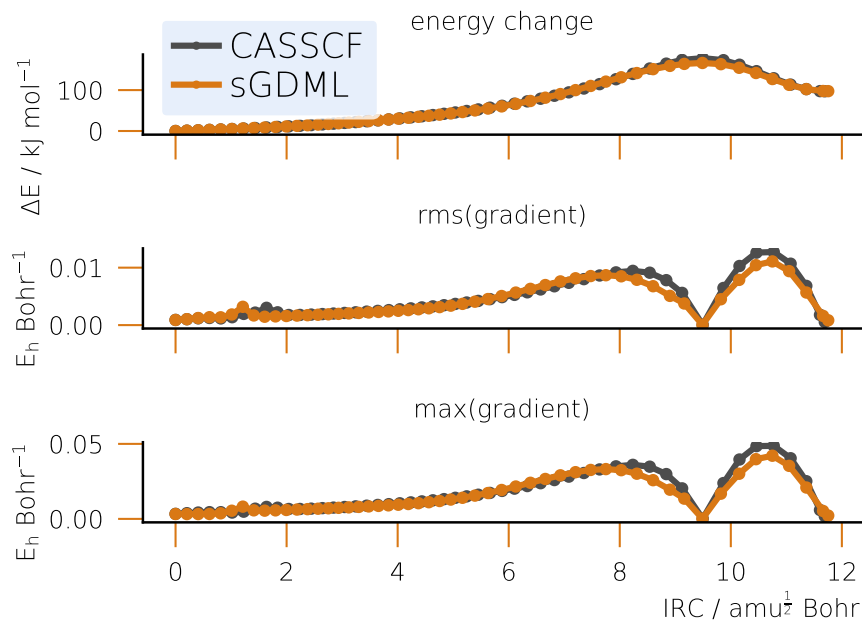


Figure 4: IRC for the Bergman cyclization of enediyne: relative energies and gradient errors. The TS corresponds to the maximum energy value at approximately 9.5 value of the IRC displacement.

The successful computation of the IRC gives the first positive accuracy assessment of vibrational modes on the semi-local fitted PES: the imaginary frequency at the TS is needed to define the direction of the path. A more detailed look at vibrational frequencies reveals only semi-qualitative agreement between the sGDML and the reference CASSCF PES (see Table S1 in the SI): the differences between the frequencies reach up to approximately 200 cm^{-1} for high-frequency nodes, which is still less than 10 %.

Rate coefficients dependent on structures, vibrations and reaction barriers are good integrated indicators of the fitted PES quality. The barrier heights for the Bergman cyclization are $\Delta E_{\text{CASSCF}}^\ddagger = 194.59 \text{ kJ}$ for the reference method and $\Delta E_{\text{sGDML}}^\ddagger = 194.57 \text{ kJ}$ for the fitted PES, which are in excellent qualitative agreement. Assuming $T = 300 \text{ K}$, we obtain the following reaction rate coefficients from the conventional TST (as described in the SI, Section 1) for the two methods: $k_{\text{CASSCF}} = 3.4548 \times 10^{-22} \text{ m}^3 \text{ s}^{-1}$ for the CAS(12, 12) and $k_{\text{sGDML}} = 4.3856 \times 10^{-22} \text{ m}^3 \text{ s}^{-1}$ for sGDML. The agreement is semi-qualitative and stems

from the pre-exponential factors defined by the partition functions, which in turn depend on vibrations and structures being less accurate than the barriers.

3.2 S_N2 reaction of chloromethane with bromide

The reaction between CH_3Cl and Br^- is shown in Fig. 5, including the optimized reactant and product.

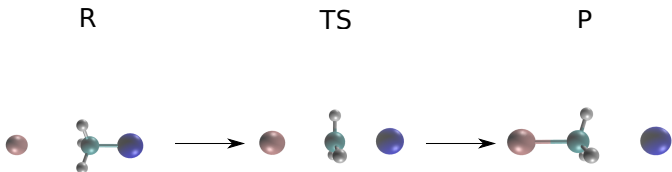


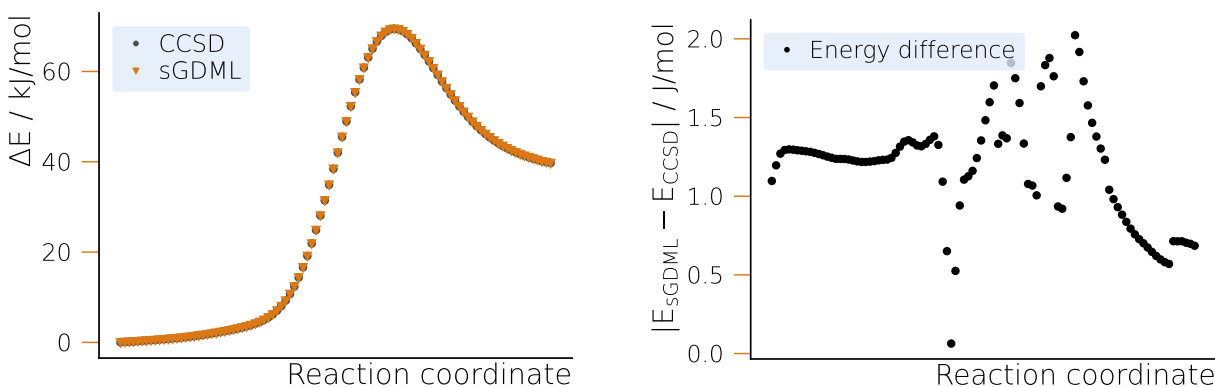
Figure 5: S_N2 reaction of chloromethane with bromide. The reactant, TS and product states are given as R, TS, and P, respectively. Elements are colored as follows: carbon (cyan), hydrogen (white), bromine (pink), chlorine (blue).

3.2.1 Model training

To generate a machine learning model, we created a data set with a total of 100 geometries separated into 50 training, 30 validation and 20 test points. The regularization parameter was set to $\lambda = 10^{-15}$ and the best length scale was found to be $\sigma = 32$. With these parameters, we obtained a model with both the MAE and RMSE being 0.0013 kJ/mol, whereas the MAE and RMSE for the forces were 0.0105 kJ/Å · mol and 0.0293 kJ/Å · mol, respectively.

3.2.2 Potential energy surface

The potential energy profiles of the S_N2 reaction for the reference method, CCSD, and sGDML are shown in Fig. 6a. The good agreement between CCSD and the sGDML fit along the (DFT) NEB path can be immediately seen in Fig. 6b. The energy difference is of similar order as for the Bergman cyclization and does not exceed 0.02 kJ/mol. However, we observe the higher errors in the TS region rather than in the vicinity of the product state.

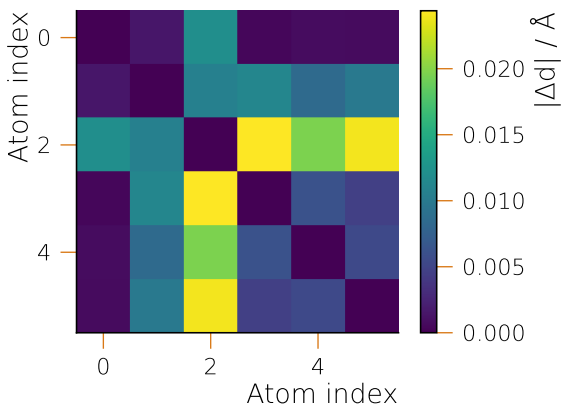


(a) Potential energy surface for CCSD and sGDML. (b) Energy differences between the learned and CCSD potential energy surface.

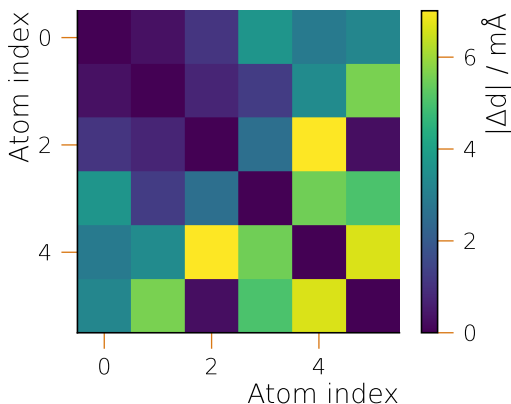
Figure 6: Potential energy profile for the S_N2 reaction of chloromethane and bromide along the optimized NEB path.

3.2.3 Geometry optimization

In Fig. 7 we compare the geometric structures of the reactant and TS obtained by sGDML and the reference method. The general agreement between the reference and fitted PES is better than for the Bergman cyclization, where the MAE never exceeds 0.025 \AA for a particular interatomic distance. For the S_N2 reaction, the better agreement is reached for the TS with the MAE staying below a value of 0.01 \AA . The largest deviation in case of the reactant state can be found for the distances between the non-bonded bromide ion (indicated by index 2) and the hydrogen atoms from the methylene group (indices 3, 4 and 5).



(a) Geometry differences (MAE) for sGDML and CCSD after performing geometry optimizations for the reactant state.



(b) Geometry differences (MAE) for sGDML and CCSD after performing geometry optimizations for the transition state.

Figure 7: Accuracy of geometric structures from the semi-local fitted PES for the S_N2 reaction of chloromethane and bromide.

3.2.4 Vibrations, intrinsic reaction coordinates and reaction rate constants

After obtaining the optimized TS, we analyze the connection between it and the basins of the reactants and products by integrating the IRC as shown in Fig. 8. On the fitted semi-local PES, the TS does connect the reactants and products by a minimum energy path, which is in qualitative agreement with the reference CCSD calculation along the entire path as indicated by the maximum and RMSE in the gradients.

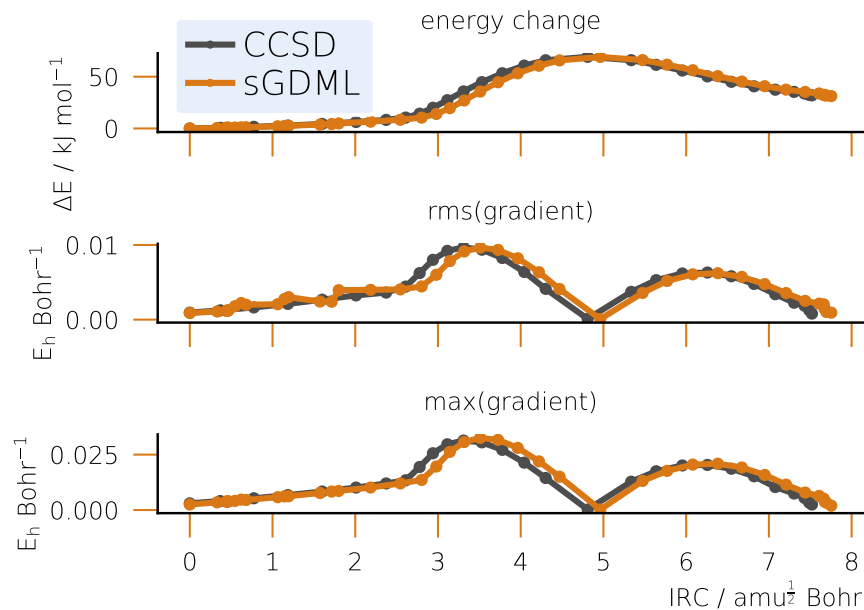


Figure 8: IRC for the S_N2 reaction of chloromethane with bromide: relative energies and gradient errors. The TS corresponds to the maximum energy value at approximately 4.8 value of the IRC displacement.

As in the previous example, successful computation of the IRC indicates the correct Hessian structure at the TS with the only imaginary eigenvalue corresponding to the same eigenvector as in the reference method. A more detailed look at vibrational frequencies reveals only qualitative agreement between the sGDML and the reference CCSD PES (see Table 2 in the SI): the differences between the frequencies reach up to approximately 300 cm^{-1} for both high- and low-frequency modes.

The barrier heights for the S_N2 reaction were identical up to the second digit: $\Delta E^\ddagger = 69.47\text{ kJ}$ for CCSD and the fitted PES. At $T = 300\text{ K}$, the CCSD reaction rate coefficient is $1.8187 \times 10^{-31}\text{ m}^3\text{s}^{-1}$, whereas this value is $2.2287 \times 10^{-32}\text{ m}^3\text{s}^{-1}$ for sGDML, which is an order of magnitude smaller than the reference method. This difference occurs due to the larger deviations in the harmonic vibrations, defining the preexponential factors in the TST equations.

4 Discussion

The most important property of the fitted semi-local PES surfaces obtained by the proposed protocol is the general stability with respect to PES exploration techniques. Indeed, for both unimolecular and bimolecular reactions geometry optimizations have converged to the stationary points, connected by physically meaningful minimum energy paths. This is achieved by the multi-scale nature of our approach.

On the one hand, the NEB driven by the cheaper method (here DFT with a PBE exchange-correlation functional) generates structures relatively close to the reactive region of the system as defined by more accurate reference electronic structure methods (here, CASSCF or CCSD). Indeed, DFT methods are known to predict sensitive geometric structures⁴³ (even if the energy barriers are not precise). This is illustrated by the S_N2 reaction studied in this work: in Fig. S1 of the SI we see that the highest energy point on the NEB path for both PBE and CCSD is located at the similar values of the reaction coordinate, although the energy barriers differ dramatically.

On the other hand, structures sampled by NEB using the cheaper method should be far enough from the minimum energy path of the reference method. The points on the true minimum energy path (approximated by NEB²⁷) have only one non-zero gradient component – the one along the path tangent direction.³ Keeping in mind that sGDML uses gradients as inputs for fitting, providing only structures on the minimum energy path would provide no information about the nature of the PES along orthogonal directions and make model very sensitive to numerical noise. Consequently, using a cheaper electronic structure method for the NEB simulation is not only computational effort saving, but also essential for the quality of the data set used to train a gradient-based ML model.

Despite qualitative agreement achieved by the semi-local fitted PES in structures, energy barriers and IRC, a more subtle property, vibrational spectrum, is computed less accurately. Although the structure of Hessian is qualitatively correct, some frequencies can differ by several hundreds of cm^{-1} . This is particularly noticeable for the S_N2 example and as a

consequence leads to a significant error (order of magnitude) in the reaction rate coefficient as compared to the reference value. This effect must have to do with a smaller number of training points (only 50) used for the model as compared to the Bergman cyclization (150 points). Another reason is the fact that the relevant PES region for the S_N2 is flatter as this for the Bergman cyclization (compare Fig. 4 and Fig. 8), one indication of which is the lower energy barrier for the former reaction. This makes finite-difference evaluation of the second derivatives of energy less reliable and requires a better PES sampling for obtaining qualitative results.

5 Conclusions and Outlook

In this work, we have proposed a multi-scale protocol for reaction mechanism studies aiming to match the accurate electronic structure theory description at the reduced computational cost. The approach involves cheaper electronic structure method to generate structures along the reaction path via the NEB method, evaluating energies and gradients for a restricted set of them with an accurate (reference) theory and fitting a semi-local reactive PES using machine learning method, sGDML. The fitted PES is then used for computing properties.

The protocol has been applied to a unimolecular (Bergman cyclization) and a bimolecular (S_N2) reactions using PBE/CASSCF and PBE/CCSD, respectively, as cheap/reference method pairs, the results being compared with those obtained on-the-fly by the reference method. Our approach achieves quantitative agreement in structure optimization for the PES stationary points, reaction energy barriers and IRC following using as little as 50-150 training points (corresponding to energy and gradient calculations with the reference method), whereas the agreement in vibrational frequencies and reaction coefficients is only (semi-)qualitative. The key to the performance of the protocol is its multi-scale character as the differences between the reference and cheap methods are essential to provide meaningful information about the reactive PES region.

The results are encouraging as important objective of mechanistic reaction study can be performed with high-level electronic structure method without prior knowledge of the TS structure (due to the application of the NEB) requiring only scarce amount of data. The protocol is simple and can be automatized for routine calculations.

At the same time, we have not considered more complex reactions with multiple steps, product branching and shallow minima. These cases would require more subtle approaches to sampling and larger amounts of training data.

Our simple protocol can be further improved by applying smart selection of training points using molecular fingerprints⁴⁴ and using methods even computationally cheaper than DFT (such as modern tight-binding, GFN2-XTB⁴⁵) for sampling structures. Moderately accurate reference methods applied here should be substituted by those providing qualitatively correct PES, such as multi-reference approaches, to match the experimental accuracy. Furthermore, the potential of different ML fitting techniques should be explored.

6 Conflicts of interest

The authors declare no conflicts of interest.

Acknowledgements

This work was supported by the German Federal Ministry of Economic Affairs and Climate Action through the PlanQK project (01MK20005H).

References

- (1) Hratchian, H. P.; Schlegel, H. B. In *Theory and Applications of Computational Chemistry*; Dykstra, C. E., Frenking, G., Kim, K. S., Scuseria, G. E., Eds.; Elsevier: Amsterdam, 2005; pp 195–249.
- (2) Truhlar, D. G.; Garrett, B. C.; Klippenstein, S. J. Current Status of Transition-State Theory. *The Journal of Physical Chemistry* **1996**, *100*, 12771–12800.
- (3) Fukui, K. Formulation of the reaction coordinate. *The Journal of Physical Chemistry* **1970**, *74*, 4161–4163.
- (4) Fernández-Ramos, A.; Miller, J. A.; Klippenstein, S. J.; Truhlar, D. G. Modeling the Kinetics of Bimolecular Reactions. *Chemical Reviews* **2006**, *106*, 4518–4584.
- (5) Helgaker, T.; Jørgensen, P.; Olsen, J. *Molecular Electronic Structure Theory*; John Wiley & Sons, LTD: Chichester, 2000.
- (6) Chamkin, A. A.; Serkova, E. S. DFT, DLPNO-CCSD(T), and NEVPT2 benchmark study of the reaction between ferrocenium and trimethylphosphine. *Journal of Computational Chemistry* **2020**, *41*, 2388–2397.
- (7) Unke, O. T.; Chmiela, S.; Sauceda, H. E.; Gastegger, M.; Poltavsky, I.; Schütt, K. T.; Tkatchenko, A.; Müller, K.-R. Machine Learning Force Fields. *Chemical Reviews* **2021**, *121*, 10142–10186.
- (8) Behler, J. Perspective: Machine learning potentials for atomistic simulations. *The Journal of Chemical Physics* **2016**, *145*, 170901.
- (9) Dral, P. O.; Barbatti, M.; Thiel, W. Nonadiabatic Excited-State Dynamics with Machine Learning. *The Journal of Physical Chemistry Letters* **2018**, *9*, 5660–5663.
- (10) Westermayr, J.; Marquetand, P. Machine Learning for Electronically Excited States of Molecules. *Chemical Reviews* **2021**, *121*, 9873–9926.

- (11) Lan, J.; Kapil, V.; Gasparotto, P.; Ceriotti, M.; Iannuzzi, M.; Rybkin, V. V. Simulating the ghost: quantum dynamics of the solvated electron. *Nature Communications* **2021**, *12*, 766.
- (12) Kapil, V.; Engel, E. A. A complete description of thermodynamic stabilities of molecular crystals. *Proceedings of the National Academy of Sciences* **2022**, *119*, e2111769119.
- (13) Gartner, T. E.; Piaggi, P. M.; Car, R.; Panagiotopoulos, A. Z.; Debenedetti, P. G. Liquid-Liquid Transition in Water from First Principles. *Phys. Rev. Lett.* **2022**, *129*, 255702.
- (14) Brickel, S.; Das, A. K.; Unke, O. T.; Turan, H. T.; Meuwly, M. Reactive molecular dynamics for the [Cl-CH₃-Br]- reaction in the gas phase and in solution: a comparative study using empirical and neural network force fields. *Electronic Structure* **2019**, *1*, 024002.
- (15) Ang, S. J.; Wang, W.; Schwalbe-Koda, D.; Axelrod, S.; Gómez-Bombarelli, R. Active learning accelerates ab initio molecular dynamics on reactive energy surfaces. *Chem* **2021**, *7*, 738–751.
- (16) Yang, M.; Bonati, L.; Polino, D.; Parrinello, M. Using metadynamics to build neural network potentials for reactive events: the case of urea decomposition in water. *Catalysis Today* **2022**, *387*, 143–149, 100 years of CASALE SA: a scientific perspective on catalytic processes.
- (17) de la Puente, M.; David, R.; Gomez, A.; Laage, D. Acids at the Edge: Why Nitric and Formic Acid Dissociations at Air–Water Interfaces Depend on Depth and on Interface Specific Area. *Journal of the American Chemical Society* **2022**, *144*, 10524–10529.
- (18) Young, T. A.; Johnston-Wood, T.; Zhang, H.; Duarte, F. Reaction dynamics of Diels–Alder reactions from machine learned potentials. *Phys. Chem. Chem. Phys.* **2022**, *24*, 20820–20827.

- (19) Töpfer, K.; Käser, S.; Meuwly, M. Double proton transfer in hydrated formic acid dimer: Interplay of spatial symmetry and solvent-generated force on reactivity. *Phys. Chem. Chem. Phys.* **2022**, *24*, 13869–13882.
- (20) Li, J.; Reiser, P.; Boswell, B. R.; Eberhard, A.; Burns, N. Z.; Friederich, P.; Lopez, S. A. Automatic discovery of photoisomerization mechanisms with nanosecond machine learning photodynamics simulations. *Chem. Sci.* **2021**, *12*, 5302–5314.
- (21) Young, T. A.; Johnston-Wood, T.; Deringer, V. L.; Duarte, F. A transferable active-learning strategy for reactive molecular force fields. *Chem. Sci.* **2021**, *12*, 10944–10955.
- (22) Feynman, R. P. Simulating physics with computers. *International Journal of Theoretical Physics* **1982**, *21*, 467–488.
- (23) Jones, R. R.; Bergman, R. G. p-Benzyne. Generation as an intermediate in a thermal isomerization reaction and trapping evidence for the 1,4-benzenediyl structure. *Journal of the American Chemical Society* **1972**, *94*, 660–661.
- (24) Ingold, C. *Structure and Mechanism in Organic Chemistry*; Cornell University Press, 1969.
- (25) Dong, H.; Chen, B.-Z.; Huang, M.-B.; Lindh, R. The bergman cyclizations of the enediyne and its N-substituted analogs using multiconfigurational second-order perturbation theory. *Journal of Computational Chemistry* *33*, 537–549.
- (26) Kerekes, Z.; Tasi, D. A.; Czakó, G. SN2 Reactions with an Ambident Nucleophile: A Benchmark Ab Initio Study of the CN⁻ + CH₃Y [Y = F, Cl, Br, and I] Systems. *The Journal of Physical Chemistry A* **2022**, *126*, 889–900.
- (27) Jónsson, H.; Mills, G.; Jacobsen, K. W. *Classical and Quantum Dynamics in Condensed Phase Simulations*; pp 385–404.

- (28) Perdew, J. P.; Burke, K.; Ernzerhof, M. Generalized Gradient Approximation Made Simple. *Phys. Rev. Lett.* **1996**, *77*, 3865–3868.
- (29) Weigend, F.; Ahlrichs, R. Balanced basis sets of split valence, triple zeta valence and quadruple zeta valence quality for H to Rn: Design and assessment of accuracy. *Phys. Chem. Chem. Phys.* **2005**, *7*, 3297–3305.
- (30) Aprà, E.; Bylaska, E. J.; de Jong, W. A.; Govind, N.; Kowalski, K.; Straatsma, T. P.; Valiev, M.; van Dam, H. J. J.; Alexeev, Y.; Anchell, J.; Anisimov, V.; Aquino, F. W.; Atta-Fynn, R.; Autschbach, J.; Bauman, N. P.; Becca, J. C.; Bernholdt, D. E.; Bhaskaran-Nair, K.; Bogatko, S.; Borowski, P.; Boschen, J.; Brabec, J.; Bruner, A.; Cauët, E.; Chen, Y.; Chuev, G. N.; Cramer, C. J.; Daily, J.; Deegan, M. J. O.; Dunning, T. H.; Dupuis, M.; Dyall, K. G.; Fann, G. I.; Fischer, S. A.; Fonari, A.; Früchtl, H.; Gagliardi, L.; Garza, J.; Gawande, N.; Ghosh, S.; Glaesemann, K.; Götz, A. W.; Hammond, J.; Helms, V.; Hermes, E. D.; Hirao, K.; Hirata, S.; Jacquelin, M.; Jensen, L.; Johnson, B. G.; Jónsson, H.; Kendall, R. A.; Klemm, M.; Kobayashi, R.; Konkov, V.; Krishnamoorthy, S.; Krishnan, M.; Lin, Z.; Lins, R. D.; Littlefield, R. J.; Logsdail, A. J.; Lopata, K.; Ma, W.; Marenich, A. V.; Martin del Campo, J.; Mejia-Rodriguez, D.; Moore, J. E.; Mullin, J. M.; Nakajima, T.; Nascimento, D. R.; Nichols, J. A.; Nichols, P. J.; Nieplocha, J.; Otero-de-la Roza, A.; Palmer, B.; Panyala, A.; Pirojsirikul, T.; Peng, B.; Peverati, R.; Pittner, J.; Pollack, L.; Richard, R. M.; Sadayappan, P.; Schatz, G. C.; Shelton, W. A.; Silverstein, D. W.; Smith, D. M. A.; Soares, T. A.; Song, D.; Swart, M.; Taylor, H. L.; Thomas, G. S.; Tipparaju, V.; Truhlar, D. G.; Tsemekhman, K.; Van Voorhis, T.; Vázquez-Mayagoitia, A.; Verma, P.; Villa, O.; Vishnu, A.; Vogiatzis, K. D.; Wang, D.; Weare, J. H.; Williamson, M. J.; Windus, T. L.; Woliński, K.; Wong, A. T.; Wu, Q.; Yang, C.; Yu, Q.; Zacharias, M.; Zhang, Z.; Zhao, Y.; Harrison, R. J. NWChem: Past, present, and future. *The Journal of Chemical Physics* **2020**, *152*, 184102.

- (31) Roos, B. O.; Taylor, P. R.; Sigbahn, P. E. A complete active space SCF method (CASSCF) using a density matrix formulated super-CI approach. *Chemical Physics* **1980**, *48*, 157–173.
- (32) Sun, Q.; Yang, J.; Chan, G. K.-L. A general second order complete active space self-consistent-field solver for large-scale systems. *Chemical Physics Letters* **2017**, *683*, 291–299, Ahmed Zewail (1946-2016) Commemoration Issue of Chemical Physics Letters.
- (33) Sun, Q.; Berkelbach, T. C.; Blunt, N. S.; Booth, G. H.; Guo, S.; Li, Z.; Liu, J.; McClain, J. D.; Sayfutyarova, E. R.; Sharma, S.; Wouters, S.; Chan, G. K.-L. PySCF: the Python-based simulations of chemistry framework. *WIREs Computational Molecular Science* **2018**, *8*, e1340.
- (34) Purvis, G. D.; Bartlett, R. J. A full coupled-cluster singles and doubles model: The inclusion of disconnected triples. *The Journal of Chemical Physics* **1982**, *76*, 1910–1918.
- (35) Dunning, T. H. Gaussian basis sets for use in correlated molecular calculations. I. The atoms boron through neon and hydrogen. *The Journal of Chemical Physics* **1989**, *90*, 1007–1023.
- (36) Woon, D. E.; Dunning, T. H. Gaussian basis sets for use in correlated molecular calculations. III. The atoms aluminum through argon. *The Journal of Chemical Physics* **1993**, *98*, 1358–1371.
- (37) Wilson, A. K.; Woon, D. E.; Peterson, K. A.; Dunning, T. H. Gaussian basis sets for use in correlated molecular calculations. IX. The atoms gallium through krypton. *The Journal of Chemical Physics* **1999**, *110*, 7667–7676.
- (38) Chmiela, S.; Tkatchenko, A.; Sauceda, H. E.; Poltavsky, I.; Schütt, K. T.; Müller, K.-R. Machine Learning of Accurate Energy-conserving Molecular Force Fields. *Science Advances* **2017**, *3*, e1603015.

- (39) Chmiela, S.; Sauceda, H. E.; Müller, K.-R.; Tkatchenko, A. Towards exact molecular dynamics simulations with machine-learned force fields. *Nature Communications* **2018**, *9*, 3887.
- (40) Chmiela, S.; Sauceda, H. E.; Poltavsky, I.; Müller, K.-R.; Tkatchenko, A. sGDML: Constructing accurate and data efficient molecular force fields using machine learning. *Computer Physics Communications* **2019**, *240*, 38–45.
- (41) Sauceda, H. E.; Chmiela, S.; Poltavsky, I.; Müller, K.-R.; Tkatchenko, A. Molecular force fields with gradient-domain machine learning: Construction and application to dynamics of small molecules with coupled cluster forces. *The Journal of Chemical Physics* **2019**, *150*, 114102.
- (42) Steinmetzer, J.; Kupfer, S.; Gräfe, S. pysisyphus: Exploring potential energy surfaces in ground and excited states. *International Journal of Quantum Chemistry* **2021**, *121*, e26390.
- (43) Bursch, M.; Mewes, J.-M.; Hansen, A.; Grimme, S. Best-Practice DFT Protocols for Basic Molecular Computational Chemistry. *Angewandte Chemie International Edition* **2022**, *61*, e202205735.
- (44) Imbalzano, G.; Anelli, A.; Giofré, D.; Klees, S.; Behler, J.; Ceriotti, M. Automatic selection of atomic fingerprints and reference configurations for machine-learning potentials. *The Journal of Chemical Physics* **2018**, *148*, 241730.
- (45) Bannwarth, C.; Ehlert, S.; Grimme, S. GFN2-xTB—An Accurate and Broadly Parametrized Self-Consistent Tight-Binding Quantum Chemical Method with Multipole Electrostatics and Density-Dependent Dispersion Contributions. *Journal of Chemical Theory and Computation* **2019**, *15*, 1652–1671, PMID: 30741547.